ELSEVIER

Chemical Engineering Journal 134 (2007) 228–234

Chemical Engineering Journal

www.elsevier.com/locate/cej

Optimum dimensions of shaped steam reforming catalysts

A.P. Kagyrmanova*, I.A. Zolotarskii, E.I. Smirnov, N.V. Vernikovskaya

Boreskov Institute of Catalysis SB RAS, Pr. Akad. Lavrentieva 5, 630090 Novosibirsk, Russia

Abstract

In this paper, a theoretical optimization of shaped catalyst dimensions with technologically imposed constraints is presented for operating conditions of a typical methanol reformer. A comprehensive two-dimensional mathematical model of a single reformer tube containing physically sound correlations for heat transfer parameters of holed catalyst particles is used. Three-hole pellets and Raschig rings were used as examples. A general conclusion is made that holed steam reforming catalysts should have maximum catalyst height and minimum diameter determined by requirements of uniform catalyst packing.

Keywords: Shaped steam reforming catalyst; Heat transport; Tubular packed bed reactor

1. Introduction

Catalysts of different sophisticated shapes including multihole pellets are widely used for commercial steam reforming of natural gas and higher hydrocarbons [1]. Shaped catalysts provide superior catalyst performance due to enhanced effectiveness factors, improved heat transfer properties and low pressure drops.

Modelling of the steam reforming process has been a subject of many papers [2–4]. One- or two-dimensional dispersion models were usually applied. However, optimization of catalyst dimensions and comparative evaluations of differently shaped catalysts were hampered for lack of general correlations able to predict heat transfer properties of a fixed bed packed with shaped catalysts until recently. As it was demonstrated by Dixon et al. [5], an alternative approach based on CFD modelling can be used to solve this problem.

In our work we use the two-dimensional pseudo-homogeneous model, but apply a recently developed methodology [6,7], which allows the prediction of parameters of radial heat transfer in beds packed with holed particles of different shape. The methodology is based on a hydrodynamic model with splitting a gas flow into streams through catalyst holes and between particles, each contributing into radial heat transfer with corresponding mixing lengths. In this case, radial thermal conductivity can be well predicted without the need for any additional fitted parameter. Further constituent is the expression of the wall heat transfer coefficient via thermal conductivity by applying a model that assumes a linear variation of the radial thermal conductivity in the vicinity of the tube wall [7]. Overall, this makes it possible to carry out theoretical optimization of catalyst dimensions for different shapes.

In this paper, sizing of a shaped steam reforming catalyst is performed by optimizing methane conversion and pressure drop at operating conditions of a typical methanol plant reformer, whilst applying restrictions related to the mechanical strength of the catalyst and packing uniformity. As an example, a three-hole cylinder was considered in detail. A catalyst shaped as a Raschig ring was used as comparison. Finally, the general conclusion on shaped steam reforming catalyst sizing is proposed.

2. Radial heat transfer in a catalyst bed packed with a shaped catalyst

Before interpretation of further results, we will briefly describe the physical principles underlying the methodology used to determine the radial heat transfer parameters for holed particles [6,7].

The effective radial thermal conductivity in a fixed bed λ_r, is composed of conductivity without flow, λ_r^0, a convective constituent, λ_r^{conv} and a radiation term λ_r^{rad}.

$$\lambda_r = \lambda_r^0 + \lambda_r^{conv} + \lambda_r^{rad} \tag{1}$$

The value of λ_r^0 can be calculated using the model of Bauer and Schlunder [8], but it is usually negligible compared to λ_r^{conv}.

---

* Corresponding author. Tel.: +7 3833 397558; fax: +7 3833 3306878.
E-mail address: aigana@catalysis.ru (A.P. Kagyrmanova).

1385-8947/$ – see front matter © 2007 Elsevier B.V. All rights reserved.
doi:10.1016/j.cej.2007.03.035

Nomenclature

a_0	specific surface area of one pellet without account of holes (m^{-1})
c_p	total gas heat capacity ($J\ mole^{-1}\ K^{-1}$)
c_{pi}	heat capacity of gas component i ($J\ mole^{-1}\ K^{-1}$)
C_i	molar concentration of component i ($mole\ m^{-3}$)
d	hole diameter of the pellet (m)
d_{eq}	equivalent hydraulic diameter of the packed bed (m), $d_{eq} = 4\varepsilon_{bed}/a_0(1-\varepsilon_{bed})$, Eqs. (2), (11)
d_{hole}	characteristic mixing length of the hole (m)
d_p	diameter of equivalent-volume sphere (m)
D	outer diameter of the pellet (m)
D_{ik}	binary diffusivity ($m^2\ s^{-1}$)
D_i^{kn}	Knudsen diffusivity ($m^2\ s^{-1}$)
D_r	effective radial diffusivity in the bed ($m^2\ s^{-1}$)
D_{ri}	effective radial diffusivity in the bed of component i ($m^2\ s^{-1}$)
D_{ri}^0	diffusivity in the bed with a stagnant fluid ($m^2\ s^{-1}$)
F	surface emissivity coefficient
H	height of the pellet (m)
ΔH_j	enthalpy change in reaction j ($J\ mole^{-1}$)
i	number of gas components, $i = \overline{1,6} = CH_4, H_2O, CO, H_2, CO_2, N_2$
l	tube length coordinate (m)
N_{hole}	number of holes in the catalyst pellet
P	pressure (atm)
Pr	Prandtl number, $Pr = \nu/\lambda_{gas}$
P_0	pressure under normal conditions (atm)
Q	degree of approaching equilibrium
r	tube radius coordinate (m)
R	universal gas constant ($atm\ m^3\ mole^{-1}\ K^{-1}$)
T	temperature (K)
T_w	tube wall temperature (K)
T_0	temperature under normal conditions (K)
u_l	superficial axial gas velocity ($m\ s^{-1}$)
$\bar{u}_l$	superficial axial gas velocity ($N\ m\ s^{-1}$), $\bar{u}_l = u_l T_0 P/P_0 T$, Eqs. (A4)–(A7)
$\bar{u}_r$	superficial radial gas velocity ($N\ m\ s^{-1}$)
y_i	molar fraction of component i
$y_{i_{in}}$	inlet molar fraction of component i
Greek letters	
α	wall heat transfer coefficient ($W\ m^{-2}\ K^{-1}$)
ε	bed void fraction, $\varepsilon = \varepsilon_{bed} + \varepsilon_{hole}(1-\varepsilon_{bed})$, Eqs. (A4) and (A5)
ε_{bed}	bed void fraction for solid pellets (without account of void fraction of pellets)
ε_{hole}	void fraction of a single pellet, $\varepsilon_{hole} = N_{hole} d/D$
γ_{ij}	stoichiometric coefficient of component i in jth reaction
λ_{gas}	gas thermal conductivity ($W\ m^{-1}\ K^{-1}$)
λ_r	effective radial thermal conductivity of the bed ($W\ m^{-1}\ K^{-1}$)
μ	gas viscosity ($kg\ m^{-1}\ s^{-1}$)
ρ	radial position in pellet (m)
ρ_{gas}	gas density ($kg\ m^{-3}$)
ρ_{grain}	characteristic thickness of pellet (m), $\rho_{grain} = V/S$
σ	Stefan–Boltzmann coefficient ($W\ m^{-2}\ K^{-4}$), $\sigma = 5.7 \times 10^{-8}$
ϖ_j	apparent reaction rate ($mole\ m^{-3}\ s^{-1}$)
ω_j	rate of the jth reaction ($mole\ m^{-3}\ s^{-1}$)
Π	permeability coefficient

The radiation part of radial thermal conductivity in Eq. (1) is defined as [9]:

$$\lambda_r^{rad} = 2F\sigma T^3 d_{eq} \tag{2}$$

At reforming conditions, the convective term λ_r^{conv} is dominant with a small contribution from radiation. In general, λ_r^{conv} is proportional to the gas velocity, u_l and the length of flow mixing and depends on the tube-to-particle diameter ratio, particularly for cylinders [10]:

$$\lambda_r^{conv} = \frac{\lambda_{gas}}{k} Re\,Pr; \quad k = \frac{8}{1.78}\left[2 - \left(1 - \frac{2}{D_{tube}/d_p}\right)^2\right] \tag{3}$$

Prediction of the effective radial thermal conductivity becomes more complicated when holed particles are used. In Ref. [6] we have suggested a hydrodynamic model which considers gas flow through catalyst holes and between particles separately. Mean velocities of these flows are related to the superficial velocity u_l through a mass balance. Furthermore, assuming that the pressure drop of gas flow through catalyst holes and between particles is the same that particles are packed with a uniform distribution of the angle between the axis of the reactor tube and that of the particles, θ, we obtain a set of algebraic Eq. (4). After solving this set of equations, the mean gas velocities around the particle (u_{out}) and in the particle holes (u_{hole}) are obtained (Fig. 1).

$$\begin{cases} u_l = u_{out}\varepsilon_{bed} + u_{hole}(\varepsilon_{hole}(1-\varepsilon_{bed})) \\ g_1 u_{hole} + g_2 u_{hole}^2 = \dfrac{\Delta P}{\langle\cos\theta\rangle H} = f_1 u_{out} + f_2 u_{out}^2 \end{cases} \tag{4}$$

Here, ΔP is the pressure drop over the distance $\langle\cos\theta\rangle H$. The mean value of $\langle\cos\theta\rangle$ is $2/\pi$. The coefficients g_1, g_2 correspond to the pressure drop in channels of different form [11], while f_1, f_2 are the coefficients of the Ergun equation [12]:

$$g_1 = \frac{16\pi\mu}{d^2}; \qquad g_2 = \frac{1.75\pi\rho_{gas}}{4H}\left(1 - \frac{\varepsilon_{hole}}{N_{hole}}\right) \tag{5}$$

$$f_1 = \frac{150\mu}{d_p^2}\left(\frac{1-\varepsilon_{bed}}{\varepsilon_{bed}}\right)^2; \qquad f_2 = \frac{1.75\rho_{gas}}{d_p}\frac{(1-\varepsilon_{bed})}{\varepsilon_{bed}} \tag{6}$$

These equations can be used to calculate a pressure drop in a fixed bed packed by shaped particles as well.

Due to these two parallel routes for heat mixing, the convective part of the radial thermal conductivity in the fixed bed core

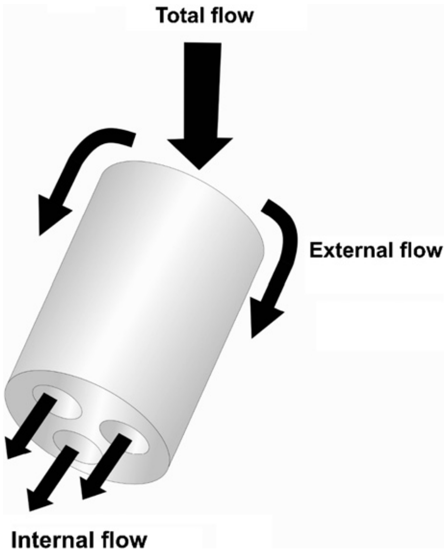

Fig. 1. Effect of "gas flow sharing" in a three-hole cylinder.

can be defined as:

$$\lambda_{\mathrm{r}}^{\mathrm{conv}} = \frac{\lambda_{\mathrm{gas}}}{k}[\varepsilon_{\mathrm{bed}} Re_{\mathrm{out}} + \varepsilon_{\mathrm{hole}}(1-\varepsilon_{\mathrm{bed}}) Re_{\mathrm{hole}}] Pr \tag{7}$$

where Reynolds numbers Re_{out} and Re_{hole} are expressed in terms of corresponding velocities and mixing length:

$$Re_{\mathrm{out}} = \frac{d_{\mathrm{p}} u_{\mathrm{out}}}{\nu}; \qquad Re_{\mathrm{hole}} = \frac{d_{\mathrm{hole}} u_{\mathrm{hole}}}{\nu} \tag{8}$$

$$d_{\mathrm{p}} = D\sqrt[3]{\frac{3}{2}\frac{H}{D}}; \qquad d_{\mathrm{hole}} = 2\langle\cos\theta\rangle \left[H + D\left(1 - \frac{1}{\sqrt{N_{\mathrm{hole}}}}\right)\right] \tag{9}$$

Effective radial diffusivity in the bed is defined similarly to the effective radial thermal conductivity:

$$D_{\mathrm{r}i} = D_{\mathrm{r}i}^{0} + \frac{\nu}{k}[\varepsilon_{\mathrm{bed}} Re_{\mathrm{out}} + \varepsilon_{\mathrm{hole}}(1-\varepsilon_{\mathrm{bed}}) Re_{\mathrm{hole}}] \tag{10}$$

Since the effective radial diffusivity in the bed $D_{\mathrm{r}i}$ is mainly determined by its convective constituent, which is the same for all components, we will take the same D_{r} equal to $D_{\mathrm{r}i}$ for methane.

In Ref. [7] we have shown that the model with a linear variation of radial thermal conductivity λ_{r} in the vicinity of the tube wall allows predicting realistic gas phase temperatures profiles for differently shaped particles in the wide range of Reynolds numbers and tube-to-particle diameter ratios. In this case, a heat transfer coefficient between a tube wall and a catalyst bed α can be determined with some assumptions as [7]:

$$\alpha = \frac{\lambda_{\mathrm{r}}}{d_{\mathrm{eq}}[\ln(\lambda_{\mathrm{r}}/\lambda_{\mathrm{gas}}) - 1]} \tag{11}$$

The above approach does not require any additional empirical parameter for the description of heat transfer in a packed bed with shaped particles.

3. Methodology for shaped catalyst sizing

3.1. Optimization criteria and particle geometry restrictions

The following optimization criteria may be used for steam reforming catalyst sizing

the maximum methane conversion;
the minimum of the highest tube wall temperature;
the minimum pressure drop along the catalyst bed.

We regard first two criteria as interrelated because both the maximum methane conversion and the minimum tube wall temperature are achieved by intensification of heat transfer from the tube wall to the catalyst bed and the apparent reaction rate. Thus, in order to apply not overcomplicated model of a steam reformer with constant tube wall temperature, we will optimize methane conversion at some fixed tube length and pressure drop.

Efficiency and safety of the steam reforming process depend on some other matters. Specifically, nonuniform catalyst packing results in maldistribution of gas flow through reformer tubes and a risk of tubes overheating. According to Ref. [13], the following inequalities should be fulfilled to provide uniform packing of cylindrical particles:

$$\frac{D_{\mathrm{tube}}}{H} \geq 5, \quad \frac{D_{\mathrm{tube}}}{D} \geq 5, \quad 0.75 \leq \frac{H}{D} \leq 1.5 \tag{12}$$

These relations are considered as restrictions for catalyst sizing.

Then, poor catalyst strength may result in catalyst damage and dust formation, thereby worsening reformer performance and shortening catalyst lifetime. Thus, catalyst strength should be kept constant during an optimization procedure. It is known from the resistance of materials, that generatrix crushing strength of a holed cylindrical particle depends on the hole diameter to outer diameter ratio d/D. It means that variation of height H and outer diameter D of the particle does not alter the mechanical strength of the catalyst, as long as ratio d/D is kept constant and the material properties are not affected.

3.2. Simulation procedure

Reformer simulations were performed by using the previously described mathematical model of a single reformer tube combined with a model of catalyst pellet [14]. This comprehensive two-dimensional pseudo-homogeneous model accounts for heat transfer from the tube wall to the catalyst bed and, heat conduction and diffusion in radial direction. Steam reforming reaction kinetics as developed by Xu and Froment [15] and the dusty gas model [16] were adopted for modelling catalyst pellets and apparent reaction rates. The catalyst activity was assumed to be 0.125 times the value reported in Ref. [15] to approach typical commercial catalyst properties. The full set of model equations is given in Appendix A. The detailed derivation of the model, computational methods and model numerical analysis were presented in Ref. [14].

Table 1
Operating conditions and catalyst parameters used in the modelling

Inlet gas temperature (°C)	520
Inlet pressure (atm)	25
Tube length (m)	12
Inlet tube diameter (m)	0.100
Feed per tube (N m^3/h)	299
Tube wall temperature (°C)	880
Inlet gas composition (vol.%)	
CH_4	24.0
H_2O	73.0
CO	1.5
H_2	1.2
CO_2	0.02
N_2	0.28
Catalyst characteristics	
Density (kg/m^3)	2030
Permeability	0.168
Mean pore radius (Å)	5000
Surface emissivity	0.85

Process parameters applied in this work correspond to a typical methanol reformer (Table 1). Simulations were performed assuming a constant tube wall temperature. Here, we present results for catalysts shaped as three-hole cylindered and as Raschig rings. The holes in a three-hole cylinder were placed such that the wall thickness' between the holes and between a hole and the outer surface was the same. Their diameter is defined from the ratio $d/D = 0.30$, which corresponds to $\varepsilon_{\text{hole}} = 0.26$. This ratio provides the same mechanical strength of three-hole particles as that for Raschig rings with $d/D = 0.47$ (corresponding to commercial catalysts). Since the inner diameter of the reformer tube is 100 mm, the studied ranges of dimensions were $D = 5$–20 mm and $H = 5$–20 mm. The following correlation for the fixed bed was applied [17]:

$$\varepsilon_{\text{bed}} = 0.36 + 0.1\frac{d_{\text{p}}}{D_{\text{tube}}} + 0.7\left(\frac{d_{\text{p}}}{D_{\text{tube}}}\right)^2 \qquad (13)$$

4. Results and discussions

Figs. 2 and 3 show the effect of three-hole cylinder dimensions on the heat transfer parameters λ_{r} and α. Catalyst height H and diameter D have the same effect on radial thermal conductivity λ_{r}. Increasing them leads to an increase of λ_{r} according to Eqs. (1), (2), (7)–(9).

The effect of catalyst dimensions on a wall heat transfer coefficient α has a more complicated character (Fig. 3). α monotonically decreases with the growth of D but has an opposite trend from the height H in the range of practical interest with $D < 13$ mm. At $D > 13$ mm dependence of α from H is divergent. This effect is caused by redistribution of gas flow through holes and around particles according to the mathematical model, as is shown in Fig. 4. An increase of the particle height H results in a raise of internal gas flow share, which enhances the radial heat conductivity. This effect is more pronounced than that of an increase of d_{eq} and finally results in increase of tube wall heat transfer coefficient according to Eq. (11).

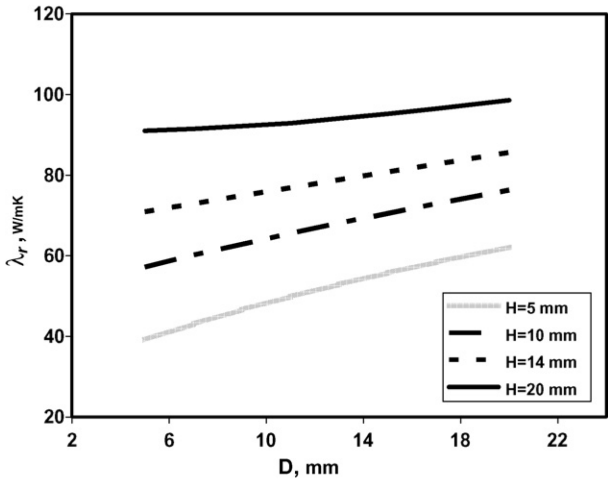

Fig. 2. Effect of three-hole cylinder dimensions on radial heat conductivity.

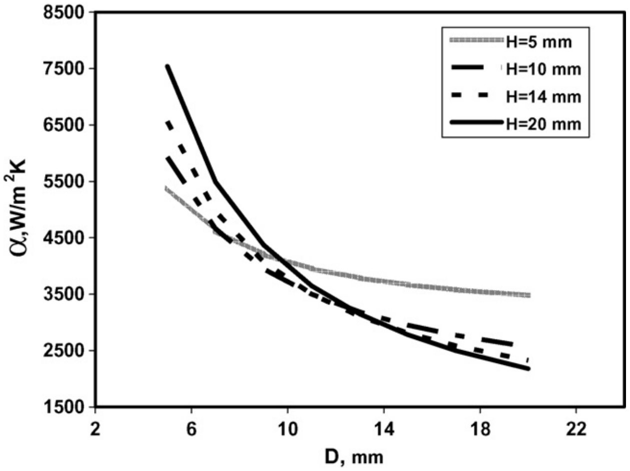

Fig. 3. Effect of three-hole cylinder dimensions on heat transfer coefficient from the tube wall to the catalyst bed.

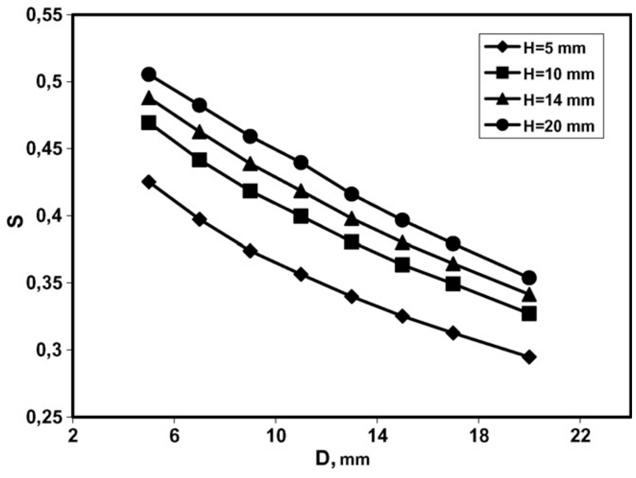

Fig. 4. Effect of three-hole cylinder dimensions on a share of gas flow through holes ($S = u_{\text{hole}}(\varepsilon_{\text{hole}}(1 - \varepsilon_{\text{bed}}))/u_{\text{l}}$).

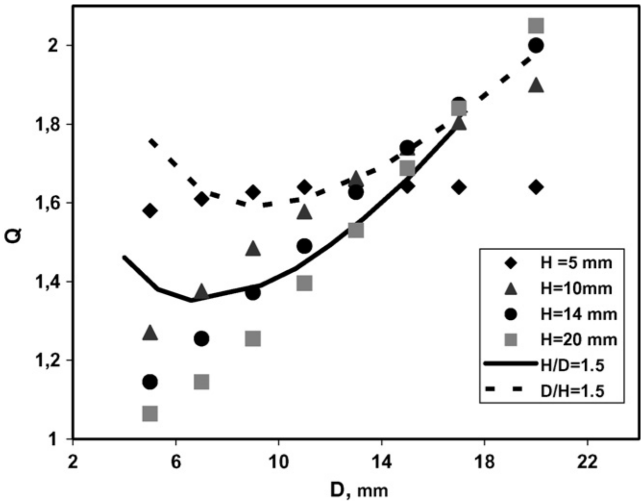

Fig. 5. Effect of three-hole cylinder dimensions on distance from equilibrium (Q) at the tube length $l = 2.4$ m.

Since steam reforming process is characterized by a strong intraparticle diffusion limitation, the effectiveness factor is practically proportional to the geometric surface area of pellet. Therefore, it is reduced if the height or diameter of the particles is increased.

Such complex effects of catalyst dimensions on heat transfer parameters and catalyst effectiveness factor disable to make a choice of catalyst sizes a priory. But simulation reveals effects of catalyst dimensions on optimization criteria as shown in Figs. 5 and 6. The methane conversion is characterized here by the ratio of the methane concentration at a fixed bed tube length ($l = 2.4$ m) and the equilibrium concentration at the tube wall temperature, named as distance from equilibrium (Q). As it was explained earlier, the ratio d/D was kept 0.3 in all calculations.

As can be seen in Figs. 5 and 6, increasing of the particle diameter D results in a decrease of both methane conversion and pressure drop along the bed, as is to be expected. The situation with the height H is different and more complicated. An increase of H results in a rise of the methane conversion and a reduction of the pressure drop over the catalyst bed, except for the range with large particles with $D > 13$ mm. In this range, the relation between α and H is divergent due to redistribution of gas flow through holes and around particles. Since process performance is more sensitive to α than to λ_r, this effect strongly determines methane conversion curves shown in Fig. 5. Namely, an increase of H does not decrease the conversion at $D > 13$ mm inspite of a drop in effectiveness factor. An increase of the outer diameter D results in a reduction of the pressure drop, but at the same time the methane conversion decreases considerably.

Therefore, the height to outer diameter ratio H/D of the optimized catalyst should be as large as allowed, namely 1.5. Solid lines in Figs. 5 and 6 correspond to the maximum acceptable $H/D = 1.5$ and dashed lines to $D/H = 1.5$. Since the methane conversion changes slightly along the line $H/D = 1.5$ in comparison with the pressure drop, optimal catalyst dimensions are mainly determined by pressure drop dependence and restricted by maximum catalyst height (20 mm). Therefore, the optimum dimensions of the three-hole cylinder catalyst are: $H = 20$ mm; $D = 13.3$ mm; $d = 3.9$ mm.

Figs. 7 and 8 show the effect of the catalyst dimensions on the optimization criteria when the catalyst is shaped as a Raschig rings with $d/D = 0.47$. The results are qualitatively similar to those obtained for three-hole cylinders, but conversion is less for Raschig rings. The reason of this is that the heat transfer coefficient, the effective radial conductivity and the effectiveness factor are higher for three-hole cylinders. Despite the larger hole diameters, the pressure drop over the bed of Raschig rings is slightly higher due to the smaller total void fraction.

Similarly to the previous case, the optimum dimensions of the Raschig ring catalyst may be chosen as $H = 20$ mm; $D = 13.3$ mm; $d = 6.25$ mm. Comparing with the three-hole cylinders with the same height and outer diameter, the Raschig ring catalyst provides 1.13 times less heat transfer coefficient, 1.16 times less effective radial thermal conductivity and 1.34 times smaller effectiveness factor. As a result, the distance from

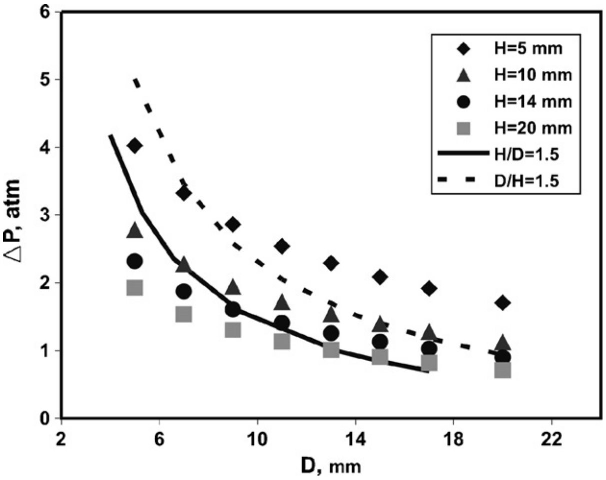

Fig. 6. Effect of three-hole cylinder dimensions on pressure drop over the whole tube length ΔP.

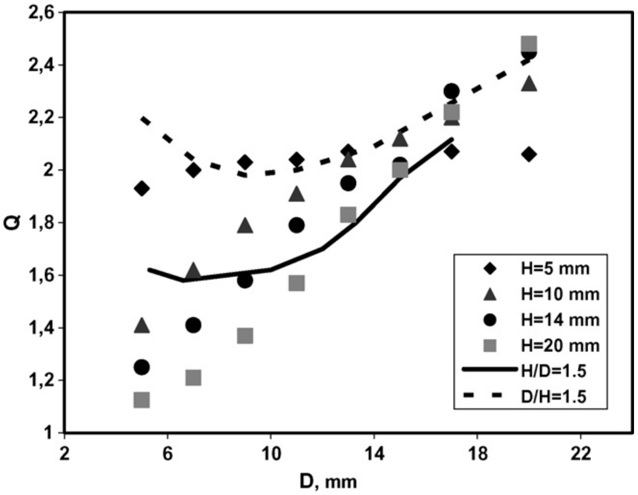

Fig. 7. Effect of Raschig ring dimensions on distance from equilibrium (Q) at the tube length $l = 2.4$ m.

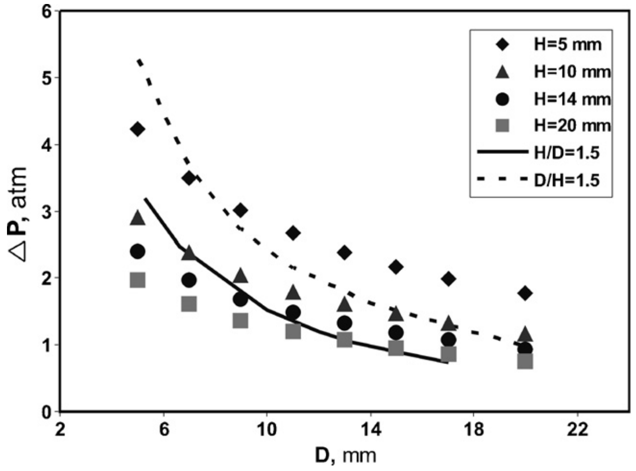

Fig. 8. Effect of Raschig ring dimensions on pressure drop over the whole tube length ΔP.

equilibrium is 1.16 times larger. Pressure drop is 1.04 times higher for optimized Raschig rings. Larger distance from equilibrium signifies smaller conversion and correspondingly higher tube wall temperature in a real process.

Similar trends were obtained for catalysts of other shapes, such as multihole cylinders, trilobes and wagon wheels, namely that the catalyst height should be maximized, while the diameter should be kept as small as possible.

5. Conclusions

Based on the results obtained it is possible to draw some general conclusions for a broad family of steam reforming catalysts shaped as holed cylinders. Catalyst height and diameter have an opposite effect on the methane conversion (intensity of heat transfer from a tube wall). Height rise and diameter reduction are favourable for the process intensification, whilst pressure drop decreases with enlarging of both sizes. Therefore, it is recommended to choose the maximum allowable catalyst height and the minimum allowable outer diameter, restricted by requirements of uniform tube packing. The size of the holes in the catalyst pellets is set of constraints on the catalyst strength.

It is demonstrated here that application of the methodology developed in Refs. [6,7] and the prediction of radial heat transfer parameters in tubular packed beds of holed particles allow a theoretical prediction of the optimum catalyst shape.

Appendix A. Mathematical model of a steam reformer tube

Catalyst pellet model:

$$\frac{\partial}{\partial\rho}\left(D^*_{\mathrm{r}i}\frac{\partial C_i}{\partial\rho}\right)-\frac{RT}{P}\frac{\partial}{\partial\rho}(V_i^*C_i)=\sum_{j=1}^{3}\gamma_{ij}\omega_j,$$

$$i=\overline{1,5},\quad C_{N_2}=\frac{P}{RT}-\sum_{i=1}^{5}C_i \tag{A1}$$

where

$$D^*_{\mathrm{r}i}=\frac{\Pi}{(RT/P)\sum_{k=1}^{6}(C_k/D_{ik})+(1/D_i^{\mathrm{kn}})}$$

is a generalized diffusivity of a component i,

$$V_i^*=\frac{(RT/P)\sum_{i=1}^{6}(J_i/D_{ik})}{(RT/P)\sum_{i=1}^{6}(C_i/D_{ik})+(1/D_i^{\mathrm{kn}})}$$

is a hydrodynamic velocity of a component i.

The molar flux of component i is defined as:

$$J_i=\int_0^{\rho}\sum_{j=1}^{3}\gamma_{ij}\omega_j\,\mathrm{d}\rho \tag{A2}$$

Boundary conditions:

$$\rho=0:\frac{\partial C_i}{\partial\rho}=0;\qquad \rho=\rho_{\mathrm{grain}}:C_i=\frac{P}{RT}y_i,\quad i=\overline{1,5}$$

The apparent reaction rates of a catalyst pellet are defined as:

$$\varpi_j=\frac{1}{\rho_{\mathrm{grain}}}\int_0^{\rho_{\mathrm{grain}}}\omega_j(\rho)\,\mathrm{d}\rho \tag{A3}$$

Tube model:

Mass and heat balance equations:

$$\frac{P_0}{RT_0}\frac{\partial(\bar{u}_1y_i)}{\partial l}+\frac{1}{r}\frac{P_0}{RT_0}\frac{\partial}{\partial r}(r\bar{u}_{\mathrm{r}}y_i)-\frac{1}{r}\frac{\partial}{\partial r}\left(r\frac{PD_{\mathrm{r}}}{RT}\frac{\partial y_i}{\partial r}\right)=\sum_j(1-\varepsilon)\gamma_{ij}\varpi_j \tag{A4}$$

$$\frac{P_0}{RT_0}\bar{u}_1c_p\frac{\partial T}{\partial l}+\frac{P_0}{RT_0}\bar{u}_{\mathrm{r}}c_p\frac{\partial T}{\partial r}-\sum_i c_{pi}\left(\frac{\partial T}{\partial r}\right)\frac{P}{RT}D_{\mathrm{r}}\frac{\partial y_i}{\partial r}-\frac{1}{r}\frac{\partial}{\partial r}\left(r\lambda_{\mathrm{r}}\frac{\partial T}{\partial r}\right)=-(1-\varepsilon)\sum_j\Delta H_j\varpi_j \tag{A5}$$

Equations for superficial axial and radial velocities:

$$\frac{\partial\bar{u}_1}{\partial l}=\frac{2RT_0}{(D_{\mathrm{tube}}^2/4)P_0}\int_0^{D_{\mathrm{tube}}/2}\sum_i\sum_j r(1-\varepsilon)\gamma_{ij}\varpi_j\,\mathrm{d}r \tag{A6}$$

$$\bar{u}_{\mathrm{r}}=-\frac{RT_0}{P_0r}\int_r^{D_{\mathrm{tube}}/2}(1-\varepsilon)r\sum_i\sum_j\gamma_{ij}\varpi_j\,\mathrm{d}r+\frac{1}{r}\frac{\partial\bar{u}_1}{\partial l}\left(\frac{D_{\mathrm{tube}}^2}{8}-\frac{r^2}{2}\right) \tag{A7}$$

Boundary conditions:

$$\begin{aligned}
&0 \le r \le \frac{D_{\mathrm{tube}}}{2}, l = 0: && \bar{u}_{\mathrm{l}}(0,r) = \bar{u}_0; \quad T(0,r) = T_{\mathrm{in}}; \quad y_i(0,r) = y_{i_{\mathrm{in}}}, \quad i = \overline{1,6}\\
&0 \le l \le L, r = 0: && \frac{\partial y_i(l,0)}{\partial r} = 0; \quad \frac{\partial T(l,0)}{\partial r} = 0\\
&r = \frac{D_{\mathrm{tube}}}{2}: && \frac{\partial y_i(l, D_{\mathrm{tube}}/2)}{\partial r} = 0, \quad i = \overline{1,5}; \quad \bar{u}_{\mathrm{r}}\left(l, \frac{D_{\mathrm{tube}}}{2}\right) = 0; \quad \lambda_{\mathrm{r}}\frac{\partial T}{\partial r} = \alpha(T_{\mathrm{w}} - T)
\end{aligned} \tag{A8}$$

References

[1] M. Nijemeisland, A.G. Dixon, E.H. Stitt, Catalyst design by CFD for heat transfer and reaction in steam reforming, Chem. Eng. Sci. 59 (2004) 5185.

[2] J. Xu, G.F. Froment, Methane steam reforming: II. Diffusional limitations and reactor simulation, AIChE J. 35 (1989) 97.

[3] M.A. Soliman, S.S. El-Nashaie, A.S. Al-Ubaid, A. Adris, Simulation of steam reformers for methane, Chem. Eng. Sci. 43 (1998) 1801.

[4] S. Grevskott, T. Rusten, M. Hillestad, E. Edwin, O. Olsvik, Modelling and simulation of a steam reforming tube with furnace, Chem. Eng. Sci. 56 (2001) 597.

[5] A.G. Dixon, M. Nijemeisland, H. Stitt, CFD simulation of reaction and heat transfer near the wall of a fixed bed, Int. J. Chem. React. Eng. (1) (2003) 22 (Article A).

[6] E.I. Smirnov, V.A. Kuzmin, I.A. Zolotarskii, Radial thermal conductivity in cylindrical beds packed by shaped particles, Chem. Eng. Res. Des. 82 (A2) (2004) 293.

[7] E.I. Smirnov, A.V. Muzykantov, V.A. Kuzmin, A.E. Kronberg, I.A. Zolotarskii, Radial heat transfer in packed beds of spheres, cylinders and Rashig rings. Verification of model with a linear variation λ_{er} in the vicinity of the wall, Chem. Eng. J. 91 (2003) 243.

[8] R. Bauer, E.U. Schlunder, Effective radial thermal conductivity of packings in gas flow. Part II. Thermal conductivity of the packing fraction without gas flow, Int. Chem. Eng. 18 (1978) 189.

[9] M.E. Aerov, O.M. Todes, Hydraulic and Thermal Principles of Operation of Apparatuses with Fixed and Fluidized Granular Beds, Khimiya, Leningrad, 1968, p. 512 (in Russian).

[10] R. Bauer, E.U. Schlunder, Effective radial thermal conductivity of packings in gas flow. Part I. Convective transport coefficient, Int. Chem. Eng. 18 (1978) 181.

[11] J. Vortuba, O. Mikus, V. Hlavacek, J. Skrivanek, A note on pressure drop in monolithic catalyst, Chem. Eng. Sci. 29 (1974) 2128.

[12] S. Ergun, Fluid flow through packed columns, Chem. Eng. Prog. 48 (1952) 89.

[13] S. Afandizadeh, E.A. Foumeny, Design of packed bed reactors: guides to catalyst shape, size, and loading selection, Appl. Therm. Eng. 21 (2001) 669.

[14] A.P. Kagyrmanova, I.A. Zolotarskii, N.V. Vernikovskaya, E.I. Smirnov, V.A. Kuzmin, N.A. Chumakova, Modeling of steam reforming of natural gas with shaped catalyst, Theor. Found. Chem. Eng. 40 (2006) 155 (in Russian).

[15] J. Xu, G.F. Froment, Methane steam reforming, methanation and water–gas shift: I. Intrinsic kinetics, AIChE J. 35 (1989) 88.

[16] E.A. Mason, A. Malinauskas, Gas Transport in Porous Media: The Dusty Gas Model, Elsevier, Amsterdam, 1983.

[17] A. Dixon, Correlations for wall and particle shape effects on fixed bed bulk voidage, Can. Chem. Eng. 66 (1988) 705.